

Effective Abelian and non-Abelian gauge potentials in cavity QED

Jonas Larson^{1,*} and Sergey Levin²

¹*NORDITA, 106 91 Stockholm, Sweden*

²*St-Petersburg State University, 198504 St-Petersburg, Russia*

(Dated: November 21, 2018)

Cavity QED models are analyzed in terms of field quadrature operators. We demonstrate that in such representation, the problem can be formulated in terms of effective gauge potentials. In this respect, it presents a completely new system in which gauge fields arise, possessing the advantages of purity, high control of system parameters as well as preparation and detection methods. Studying three well known models, it is shown that either Abelian or non-Abelian gauge potentials can be constructed. The non-Abelian characteristics are evidenced via numerical simulations utilizing experimental parameters.

PACS numbers: 45.50.Pq, 03.65.Vf, 31.50Gh

Introduction. – Gauge fields naturally arise when describing subatomic interactions. Ranging from classical electromagnetism [1] to quantum Hall systems [2] and more recently cold atoms in optical lattices [3], gauge theories have deepened our understanding for fundamental processes in AMO physics. The simplest and most familiar example is found when considering a charge particle in an electromagnetic field. In this case, the gauge theory is Abelian, as the vector components of the gauge field mutually commute. For non-Abelian gauge fields, on the other hand, the vector field components are non commuting operators. In general, time-ordering then becomes important, leading to novel phenomena. With the experimental progress in especially AMO physics, non-Abelian gauge structures have drawn great interest in recent years.

Wilczek and Zee showed that by adiabatically changing a Hamiltonian, possessing degenerate states, effective non-Abelian gauge potentials can be achieved [4]. Indeed, the appearance of gauge potentials for adiabatic evolution had been demonstrated some years prior by Mead and Truhlar studying molecular systems [5]. Here, adiabaticity is a result from separation of fast electronic and slow nuclear motions in the molecule, *i.e.* the Born-Oppenheimer approximation. Thus, the gauge potential derives from intrinsic spatial evolution [6] and not from explicit time-dependence as utilized in [4]. Similar situations emerge for cold atoms interacting with spatially varying light fields [7]. The center of mass motion of the atom induces an effective gauge potential, and by considering a coupled four-level tripod atomic system, Ruseckas *et al.* presented a model which exhibits a non-Abelian gauge structure [8]. The advantage of this cold atom model is the high controllability of system parameters as well as efficient preparation and detection methods.

In this Letter we present a completely different system in which effective gauge potentials appear, with the same assets as for the cold atom model, *i.e.* purity, coherent control of system parameters, preparation, and detection. In particular, we consider a single few-level

atom (could be a true atom or a quantum dot representing an artificial atom) interacting with one or two quantized cavity modes. By expressing the field in terms of its quadrature operators, the structure of the Hamiltonian becomes similar to the ones encountered in molecular models. In other words, an adiabatic diagonalization renders effective gauge fields. This is demonstrated by analyzing three well known models, where two are endowed with non-Abelian properties.

Since two decades, cavity quantum electrodynamics (QED) with single or few atoms has delivered some of the most striking experimental results on pure quantum phenomena [9]. Among others, entanglement generation [10], the quantum measurement problem and the quantum-classical transition [11], and verification of the graininess of the quantized electromagnetic field [12]. Cavity QED has attracted even more interest in recent years due to the realization of coherent coupling of single quantum dots [13] or Bose-Einstein condensates [14] to a cavity mode. These experiments pave the way for the possibility of reaching a super-strong coupling regime of cavity QED.

The general form of our Hamiltonian reads

$$H = H_f + H_a + H_I \quad (1)$$

where

$$\begin{aligned} H_f &= \hbar \sum_k \omega_k \hat{a}_k^\dagger \hat{a}_k, \\ H_a &= \sum_{j=1}^N E_j |j\rangle \langle j|, \\ H_I &= \sum_j \vec{d}^{(j)} \cdot \vec{E}(\mathbf{x}). \end{aligned} \quad (2)$$

Here, ω_k is the k 'th field mode frequency, \hat{a}_k^\dagger (\hat{a}_k) the creation (annihilation) photon operator of mode k , E_j the energy of atomic level j , N the number of atomic states, $\vec{d}^{(j)}$ the dipole operator for atomic transition j , and $\vec{E}(\mathbf{x})$ is the electric cavity field. In the dipole approximation

we set $\mathbf{x} = 0$, and the field can be written as

$$\bar{E} = \sum_k \bar{\varepsilon}_k \mathcal{E}_k i \left(\hat{a}_k - \hat{a}_k^\dagger \right), \quad (3)$$

where $\bar{\varepsilon}_k$ is the polarization vector for mode k and \mathcal{E}_k the corresponding field amplitude. Moreover, the components of the dipole moment become $d_\alpha^{(j)} = -e|j\rangle\langle j|\alpha|j+1\rangle\langle j+1| + h.c.$ with $\alpha = x, y, z$, e the electron charge, and $h.c.$ is the Hermitian conjugate. For our purpose, it is convenient to express the Hamiltonian in its field quadrature operators

$$\hat{X}_k = \frac{1}{\sqrt{2}} \left(\hat{a}_k + \hat{a}_k^\dagger \right), \quad \hat{P}_k = \frac{i}{\sqrt{2}} \left(\hat{a}_k - \hat{a}_k^\dagger \right), \quad (4)$$

obeying the canonical commutation relations; $[\hat{X}_k, \hat{P}_{k'}] = i\delta_{kk'}$. The field quadrature operators (4) are easily measured experimentally. Indeed, the ENS group of S. Haroche recently presented experimental results where the full phase space distribution of a cavity mode was assessed [15]. In terms of (4), the Hamiltonian (1) takes the form

$$H = \hbar \sum_k \omega_k \left(\frac{\hat{P}_k^2}{2} + \frac{\hat{X}_k^2}{2} \right) + \sum_{j=1}^N E_j |j\rangle\langle j| - \sum_{j=1}^N \sum_k \bar{d}^{(j)} \cdot \bar{\varepsilon}_k g_{jk} \hat{P}_k, \quad (5)$$

where g_{jk} is the effective atom-field coupling between the transition j and the mode k . The general form of the Hamiltonian (5) works as a starting point to analyze more specific cavity QED models.

Rabi model. – The simplest non-trivial situation considers a single cavity mode interacting with one atomic transition. Experimentally, such idealized situations are accessible by utilizing high- Q cavities with well resolved resonance frequencies ω_k , see for example Refs. [9, 10, 11, 12]. For this model we leave out the indices j and k . Introducing the Pauli matrices $\hat{\sigma}_x = |2\rangle\langle 1| + |1\rangle\langle 2|$, $\hat{\sigma}_y = -i|2\rangle\langle 1| + i|1\rangle\langle 2|$, and $\hat{\sigma}_z = |2\rangle\langle 2| - |1\rangle\langle 1|$, and without loss of generality assuming that $\bar{d} \cdot \bar{\varepsilon}$ is purely real, we obtain the Rabi Hamiltonian

$$H_{Rabi} = \hbar\omega \left(\frac{\hat{P}^2}{2} + \frac{\hat{X}^2}{2} \right) + \frac{\hbar\Omega}{2} \hat{\sigma}_z - \hbar g \hat{\sigma}_x \hat{P}. \quad (6)$$

Here, g is the vacuum Rabi frequency, giving the effective atom-field coupling, and we have chosen our zero energy such that $E_1 = -\hbar\Omega/2$ and $E_2 = \hbar\Omega/2$.

We note that the Hamiltonian can be rewritten as

$$H_{Rabi} = \hbar\omega \left(\frac{(\hat{P} - \hat{A})^2}{2} + \frac{\hat{X}^2}{2} \right) + \frac{\hbar\Omega}{2} \hat{\sigma}_z + \hat{\Phi}, \quad (7)$$

where we have introduced the scaled gauge potential $\hat{A} = \frac{g}{\omega} \hat{\sigma}_x$ and the scalar potential $\hat{\Phi} = -\hbar \frac{g^2}{2\omega}$. Under a unitary

transformation of the state vector $\Psi(\hat{X}, t)$,

$$\Psi(\hat{X}, t) \rightarrow U^\dagger(\hat{X}, t) \Psi(\hat{X}, t), \quad (8)$$

the gauge and scalar potential transforms accordingly

$$\begin{aligned} \hat{A} &\rightarrow U^\dagger(\hat{X}, t) \hat{A} U(\hat{X}, t) - U^\dagger(\hat{X}, t) \frac{\partial}{\partial \hat{X}} U(\hat{X}, t), \\ \hat{\Phi} &\rightarrow U^\dagger(\hat{X}, t) \hat{\Phi} U(\hat{X}, t) - i\hbar U^\dagger(\hat{X}, t) \frac{\partial}{\partial t} U(\hat{X}, t). \end{aligned} \quad (9)$$

The above equation demonstrates the gauge structure of the effective potentials.

It should be observed that the appearance of the effective gauge potentials results from the non-stationary dynamics of the quantized cavity field, and not from adiabatic particle motion as in earlier works on cold atoms and molecular physics [5, 6, 7, 8]. Furthermore, note that by applying the rotating wave approximation, H_{Rabi} turns into the solvable Jaynes-Cummings Hamiltonian [16] that has served as workhorse in the field of quantum optics ever since it was introduced [17]. Imposing such an approximation would make the present analysis less transparent since the atom field coupling would then depend on both \hat{P} and \hat{X} rendering complicated gauge potentials. In addition, for current quantum dot cavity QED systems, application of the rotating wave approximation is not always justified.

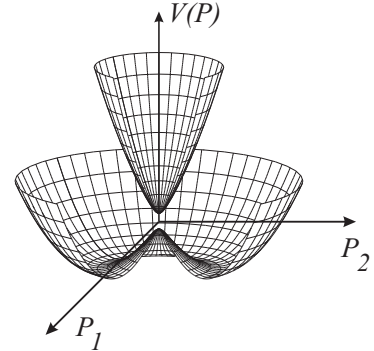


Figure 1: Effective APSs of the bimodal Rabi Hamiltonian (10) in the $g > \sqrt{\omega\Omega}$ case, where the lower APS attains the sombrero shape. The conical intersection is located at the origin, $P_1 = P_2 = 0$.

Bimodal Rabi model. – In order to acquire non-Abelian gauge potentials, additional degrees of freedom must be included. This is easily accomplished in our cavity QED setting by considering a bimodal cavity field [18]. Hence, the atom interacts simultaneously with two cavity modes. It is worth noting that experiments on bimodal cavities have been successfully demonstrated [19]. The simplest extension of the Rabi model is to keep the two-level structure of the atom and simply add one additional cavity mode. Recently, it was shown that the corresponding cavity QED model has a Jahn-Teller structure [20]. For appropriate choices of polarizations and atomic dipole

moments, one obtains the $E \times \varepsilon$ Jahn-Teller Hamiltonian which has been thoroughly studied in especially molecular physics [21]. The model possesses a conical intersection in which the adiabatic potential surfaces become degenerate. Encircling the intersection brings about a non-zero geometrical phase characterized by a gauge potential. We note that geometrical phases have been discussed in terms of cavity QED [20, 22]. These, however, do either consider the Abelian situation or Berry phases originating from a time-dependent Hamiltonian and consequently the gauge field derives from external driving rather than from intrinsic dynamical evolution.

The $E \times \varepsilon$ cavity QED Hamiltonian is given by [20]

$$H_{BR} = \hbar\omega \sum_{k=1,2} \left(\frac{\hat{P}_k^2}{2} + \frac{\hat{X}_k^2}{2} \right) + \frac{\hbar\Omega}{2} \hat{\sigma}_z - \hbar g \left(\hat{\sigma}_x \hat{P}_1 + \hat{\sigma}_y \hat{P}_2 \right). \quad (10)$$

Here, we have assumed equal mode frequencies and equal atom-field strengths. Contrary to Jahn-Teller models encountered in molecular physics, the conical intersection appears in momentum space rather than in position. In the condensed matter community, a coupling as the one in Eq. (10) is usually said to be on Rashba form [23]. The adiabatic potential surfaces (APS), defined as $V_{ad}^{\pm}(P_1, P_2) = \hbar\omega (P_1^2 + P_2^2)/2 \pm \hbar\sqrt{\Omega^2/4 + g^2(P_1^2 + P_2^2)}$, are envisaged in Fig. 1. Due to the non-zero Ω , the conical section becomes avoided. The lower APS has a sombrero shape whenever $g > \sqrt{\Omega\omega}$, otherwise a global minimum at the origin is exhibited. It follows directly from the form of the Hamiltonian (10), that the vector and scalar potentials read

$$(\hat{A}_1, \hat{A}_2) = \frac{g}{\omega} (\hat{\sigma}_x, \hat{\sigma}_y), \quad \hat{\Phi} = -\hbar \frac{g^2}{\omega}, \quad (11)$$

and since $[\hat{A}_1, \hat{A}_2] \neq 0$, the gauge potential is non-Abelian.

In a recent work [24], considering a spinor Bose-Einstein condensate, a proposal for detecting non-Abelian characteristics was put forwarded. The idea is to initialize a state, such that it is given by a fairly localized wave packet with non-zero average momentum, and then boost the wave packet either clockwise or anti-clockwise. Due to the non-Abelian structure, the two paths will render different dynamics despite the polar symmetry of the problem. To demonstrate this, we chose the atom to be initially in a superposition state $(|2\rangle - |1\rangle)/\sqrt{2}$ and the two fields to be in coherent states

$$\psi_i(P_i, 0) = \frac{1}{\sqrt{\pi}} e^{-i(\Im P_{i0})^2} e^{-iX_{i0}P_i} e^{-(P_i - P_{i0})^2/2}, \quad i = 1, 2, \quad (12)$$

where P_{i0} and X_{i0} are initial average momentum and position respectively. These are related to the initial coherent state amplitude $\alpha_{i0} = (X_{i0} + iP_{i0})/\sqrt{2}$. For the

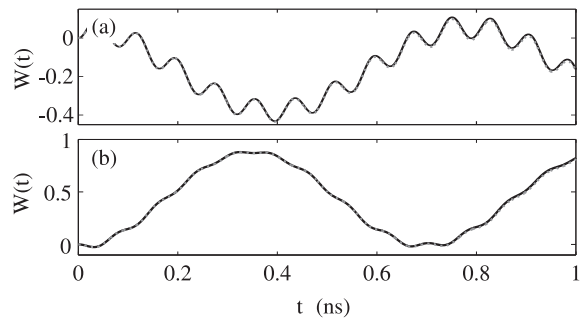


Figure 2: Time evolution of the atomic inversion for clockwise (a) and anti-clockwise (b) propagation. Solid lines display the ideal case of no losses, while for the dotted lines both cavity and atomic losses are included. The non-Abelian structure of the model is clearly visible. The system parameters are $P_{10} = 2$, $P_{20} = 0$, $X_{10} = 0$, $X_{20} = \pm 5$, $\Omega/2\pi = 6.9$ GHz, $\omega/2\pi = 5.7$ GHz, $g/2\pi = 105$ MHz, $\gamma/2\pi = 1.9$ MHz, and $\kappa/2\pi = 250$ kHz.

situation at hand, we set $P_{10} > 0$, $P_{20} = 0$, $X_{10} = 0$, and $X_{20} \neq 0$. In momentum representation, this gives an initial wave packet mainly at the lower APS located at the positive P_1 -axis and with an initial velocity perpendicular to this axis. For $X_{20} > 0$, the wave packet sets off clockwise around the origin, while $X_{20} < 0$ results in anti-clockwise evolution. Our numerical simulation utilizes the split-operator method, which gives the time-evolved wave packet at any instant of time. Solid lines of Fig. 2 presents the results for the atomic inversion, $W(t) = p_2(t) - p_1(t)$ where $p_i(t)$ is the probability of finding the atom in the state $|i\rangle$ at time t , for clockwise propagation (a) and for anti-clockwise evolution (b). The final time corresponds to approximately six roundtrips around the conical intersection. We point out that the atomic inversion can be experimentally measured up to a few percent accuracy [9]. The discrepancy between the lines of (a) and (b), evident even at very short time scales (\sim ns), is a manifestation of the underlying non-Abelian character.

A deeper understanding is obtained by studying the evolution of the fields in phase space. As for a classical harmonic oscillator, both fields will encircle the origin of phase space with, for the example of Fig. 2, radii approximately 2 and 5 respectively. The effective magnetic field deriving from the gauge potential renders a momentum dependent force. The momentum is in general different for clockwise and anti-clockwise evolution, and hence this effective Lorentz force acting on the field distributions implies slightly deviating trajectories in phase space for the two cases. This difference is the origin for the momentum-dependence of the atomic inversion seen in Fig. 2.

In realistic situations, both cavity and atomic losses come into play. We schematically take these losses into account by consider time evolution of the ef-

fective non-hermitian Hamiltonian $H_{eff} = H_{BR} - i\kappa (\hat{a}_1^\dagger \hat{a}_1 + \hat{a}_2^\dagger \hat{a}_2) - i\gamma |2\rangle\langle 2|$. Here κ and γ are the photon decay rate and the atomic spontaneous emission rate respectively. The results of such numerical simulation are given by the dotted lines of Fig. 2. The parameters used in the examples of Fig. 2 have been chosen according to the quantum dot cavity QED experiments of Ref. [13]. Due to the short interaction times of Fig. 2, losses play a minor role. The importance of losses becomes apparent only for longer time scales.

Bimodal Λ model. – Our final example considers a Λ -atom with two lower meta stable states $|1\rangle$ and $|2\rangle$ coupled to an excited state $|3\rangle$ via two cavity fields 1 and 2 respectively. Numerous theoretical works on this system have been put forward [18], and Ref. [25] presents some experimental studies of Λ cavity experiments.

The Hamiltonian for this system reads

$$H_\Lambda = \hbar\omega \sum_{k=1,2} \left(\frac{\hat{P}_k^2}{2} + \frac{\hat{X}_k^2}{2} \right) + \sum_{j=1,2,3} E_j |j\rangle\langle j| - \hbar g \left(\hat{P}_1 |3\rangle\langle 1| + \hat{P}_2 |3\rangle\langle 2| + h.c. \right), \quad (13)$$

where we have assumed that the effective atom-field couplings are real and the same between the two transitions. For degenerate lower atomic states $E_1 = E_2$, the three APSs possess a Renner-Teller intersection [26] between the lower and the middle surface and another one between the middle and the upper surface. These intersections are characterized by that the tangents of the two surfaces are the same at the degenerate point. Moreover, the Berry phase acquired by encircling a Renner-Teller intersection in position space vanishes. Here, however, the intersection is in the momentum space giving rise to a non-Abelian Berry phase in position space, where we have checked that for $E_1 = E_2$ the diagonal terms of the corresponding 3×3 geometric phase matrix are zero but some of the off-diagonal terms are indeed non-zero. If the two lower atomic states are not degenerate $E_1 \neq E_2$, both Renner-Teller intersections split into two non-avoided conical intersection.

As in the previous bimodal example, the gauge potential is non-Abelian;

$$(\hat{A}_1, \hat{A}_2) = \frac{g}{\omega} (\hat{\lambda}_4, \hat{\lambda}_6), \quad \hat{\Phi} = \hbar \frac{g^2}{3\omega} \left(1 - \frac{\sqrt{3}}{2} \hat{\lambda}_8 \right), \quad (14)$$

with $\hat{\lambda}_j$ being the Gell-Mann matrices ($\hat{\lambda}_4 = |3\rangle\langle 1| + |1\rangle\langle 3|$, $\hat{\lambda}_6 = |3\rangle\langle 2| + |2\rangle\langle 3|$, and $\hat{\lambda}_8 = (|1\rangle\langle 1| + |2\rangle\langle 2| - 2|3\rangle\langle 3|)/\sqrt{3}$).

Concluding remarks. – We have demonstrated how cavity QED models provide novel systems exhibiting artificial gauge potentials. This derives from the quantized motion of the cavity fields; the dynamics of the fields in phase space. Moreover, using numerical simulations we

showed that non-Abelian characteristics should be detectable under realistic conditions. From this rather unusual approach to cavity QED, presented in this Letter and earlier in [16, 20], it is clear that these models are very rich. We are at the moment analyzing the prospects of achieving zitterbewegung or Hall effects with cavity QED setups [27]. We hope that the current contribution will encourage experiments along these lines.

We wish to thank Prof. Erik Sjöqvist for fruitful discussions, and JL acknowledge support from the MEC program (FIS2005-04627).

* Electronic address: jolarson@kth.se

- [1] J. D. Jackson *Classical Electrodynamics* (Wiley, New York 2002).
- [2] K. V. Klitzing, *et al.*, Phys. Rev. Lett. **45**, 494 (1980).
- [3] K. Osterloh *et al.*, Phys. Rev. Lett. **95**, 010403 (2005); I. I. Satija *et al.*, Phys. Rev. Lett. **97**, 216401 (2006).
- [4] F. Wilczek and A. Zee, Phys. Rev. Lett. **52**, 2111 (1984).
- [5] C. A. Mead and D. G. Truhlar, J. Chem. Phys. **70**, 2284 (1979).
- [6] C. A. Mead, Rev. Mod. Phys. **64**, 51 (1992).
- [7] R. Dum and M. Olshanii, Phys. Rev. Lett. **76**, 1788 (1996); Y.-J. Lin, *et al.*, arXiv:0809.2976.
- [8] J. Ruseckas *et al.*, Phys. Rev. Lett. **95**, 010404 (2005).
- [9] *Cavity Quantum Electrodynamics*, edited by P. R. Berman (Academic Press, New York 2994); S. Haroche and J. M. Raimond, *Exploring the Quantum* (Oxford University Press, Oxford 2006).
- [10] E. Hagley *et al.*, Phys. Rev. Lett **79**, 1 (1997).
- [11] M. Brune *et al.*, Phys. Rev. Lett. **77**, 4887 (1996); C. J. Hood *et al.*, Science **287**, 1447 (2000).
- [12] G. Rempe and H. Walther, Phys. Rev. Lett. **58**, 353 (1987); M. Brune *et al.*, Phys. Rev. Lett. **76**, 1800 (1996).
- [13] D. I. Schuster *et al.*, Nature **445**, 515 (2007).
- [14] F. Brennecke *et al.*, Nature **450**, 268 (2007); Y. Colombe *et al.*, Nature **450**, 272 (2007).
- [15] S. Deleglise *et al.*, Nature **455**, 510 (2008).
- [16] J. Larson, Phys. Scr. **76**, 146 (2007).
- [17] E. T. Jaynes and F. W. Cummings, Proc. IEEE **51**, 89 (1963); B. W. Shore and P. L. Knight, J. Mod. Opt. **40**, 1195 (1993).
- [18] A. Messina *et al.*, J. Mod. Opt. **50**, 1 (2003).
- [19] A. Rauschenbeutel *et al.*, Phys. Rev. Lett. **64**, 050301 (2001).
- [20] J. Larson, Phys. Rev. A **78**, 033833 (2008).
- [21] H. C. Longuet-Higgins *et al.*, Proc. R. Soc. London Ser. A **244**, 1 (1958); D. R. Yarkony, Rev. Mod. Phys. **68**, 985 (1996).
- [22] I. Fuentes-Guridi *et al.*, Phys. Rev. Lett. **89**, 220404 (2002); P. Zhang *et al.*, Phys. Rev. A **71**, 042301 (2005).
- [23] Y. A. Bychkov and E. I. Rashba, J. Phys. C **17**, 6039 (1984).
- [24] J. Larson and E. Sjöqvist, arXiv:0812.1725.
- [25] M. Hennrich *et al.*, Phys. Rev. Lett. **85**, 4872 (2000); M. Hijlkema *et al.*, NATURE PHYSICS **3**, 253 (2007); M. Khudaverdyan *et al.*, arXiv:0901.3738.
- [26] T. J. Lee *et al.*, J. Chem Phys. **81**, 356 (1984).
- [27] J. Y. Vaishnav and C. W. Clark, Phys. Rev. Lett. **100**,

153002 (2008); S.-L. Zhu *et al.*, Phys. rev. Lett. **97**,
240401 (2006).